Evidence for canted antiferromagnetism in lightly doped $La_{1-x}Sr_xMnO_3$

J. Geck, B. Büchner,* M. Hücker,* R. Klingeler, and R. Gross†
II. Physikalisches Institut, Universität zu Köln, Zülpicher Str. 77, 50937 Köln, Germany

L. Pinsard-Gaudart and A. Revcolevschi
Laboratoire de Physico-Chimie des Solides, Université Paris-Sud, 91405 Orsay Cedex, France
(Received 27 November 2000; revised manuscript received 28 February 2001; published 24 September 2001)

We present magnetization measurements on lightly doped $La_{1-x}Sr_xMnO_3$ single crystals with $0.06 \leqslant x \leqslant 0.15$ in external fields up to 14 T at temperatures between 4.2 and 180 K. In contrast to the ferromagnetic behavior which is found for $x \geqslant 0.11$, the samples with $x = 0.06$ and $x = 0.09$ exhibit a pronounced hysteresis and a constant high-field susceptibility. By analyzing this particular behavior we can rule out a phase separation into ferromagnetic and antiferromagnetic regions. On the other hand, a model of a canted antiferromagnet can account for the main experimental features.

DOI: 10.1103/PhysRevB.64.144430 PACS number(s): 75.30.Vn, 75.30.Gw, 75.60.Ej, 75.25.+z

I. INTRODUCTION

In the last years the manganites have attracted renewed interest because of their rich physics and possible applications. In particular, lightly doped $La_{1-x}Sr_xMnO_3$ shows a great variety of intriguing phenomena originating from a pronounced interplay between lattice, electronic, magnetic, and orbital degrees of freedom.[1–5] As a result many phenomena like charge order,[6,7] orbital order,[8,9] and phase separation[10–12] have been recently observed in this regime of the phase diagram and discussed intensively. One of the interesting questions related to lightly doped $La_{1-x}Sr_xMnO_3$, which certainly is crucial for a deeper understanding of these materials, is how the introduced holes behave at low temperatures. At present, there is a controversial debate on whether a homogeneous phase with constant hole concentration or an inhomogeneous phase develops.[11–20] If there is a spatially inhomogeneous phase, i.e., if phase separation (PS) occurs, both antiferromagnetic and ferromagnetic areas coexist. In contrast, in the presence of a homogeneous phase a canted antiferromagnetic (CAF) spin order[19] is expected. Unfortunately, from the experimental data it usually is difficult to decide whether or not there is phase separation. For example, neutron scattering experiments revealed spatially varying magnetic properties, whereas recent NMR experiments suggest a homogenous phase.[13,15] A clear-cut discrimination is even more difficult from macroscopic properties, such as the magnetization, because in most cases the experimental observations can be explained by both an inhomogeneous or a homogeneous phase.

In this paper we present magnetization measurements on lightly doped $La_{1-x}Sr_xMnO_3$ single crystals with $x = 0.06, 0.09, 0.11, 0.125$, and 0.14. In the case of 6% and 9% strontium doping our measurements indicate the coexistence of ferro- and antiferromagnetic correlations. We present a detailed analysis of the magnetization data for the $La_{0.94}Sr_{0.06}MnO_3$ single crystal from which we can rule out an inhomogeneous phase with coexisting ferromagnetic (FM) and antiferromagnetic (AFM) regions.

II. EXPERIMENTAL TECHNIQUES

The measurements of the magnetization were performed using a vibrating sample magnetometer. The magnetometer was designed for measurements in high external fields. In order to access the temperature regime from 4.2 K up to about 200 K and magnetic fields up to 14 T a liquid helium cryostat with a superconducting solenoid was used.

The $La_{1-x}Sr_xMnO_3$ single crystals have been grown using the traveling solvent floating zone (TSFZ) method which is described in detail elsewhere.[21] As a result of the structural phase transition from a quasicubic to an orthorhombic $Pbnm$ symmetry at high temperature the crystals are twinned. This means that the [001] direction of one domain can coincide with the [110] direction of another. Moreover, the a and b axes can be interchanged, leading to six possible orientations for the different twin domains.

III. MAGNETIZATION VERSUS TEMPERATURE

Figure 1 shows the magnetization versus temperature curve of the $La_{0.94}Sr_{0.06}MnO_3$ single crystal. The curve was

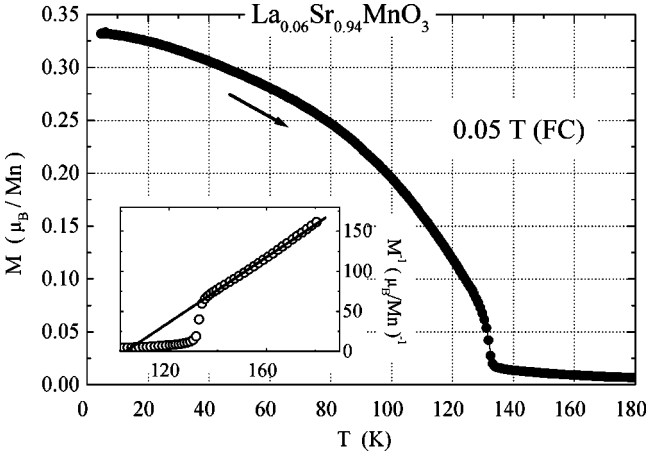

FIG. 1. FC magnetization measured at increasing temperature in an external field of 0.05 T. The inset shows the corresponding inverse magnetization vs temperature curve.

obtained by cooling down the sample from about 200 to 4.2 K in an applied magnetic field of 0.05 T [field-cooled (FC) mode[22]] and taking the data with increasing temperature. Above the magnetic transition temperature $T_C \simeq 132$ K a paramagnetic susceptibility $\chi = \partial M/\partial H|_{H=0}$ following a Curie-Weiss law with positive Curie temperature of $\Theta = (104 \pm 1.5)$ K is measured. Because Θ is proportional to the average coupling constant, the experimental observation that $0 < \Theta < T_c$ signals the presence of antiferromagnetic as well as ferromagnetic correlations. As a result of this coexistence, an unusual magnetic transition is observed at T_C, which is neither purely ferromagnetic nor purely antiferromagnetic. This is demonstrated by the inset of Fig. 1. It is evident that the inverse magnetization suddenly deviates from the expected mean-field behavior of a ferromagnet. Additional measurements of the ac susceptibility lead to the conclusion that this transition is also not a usual antiferromagnetic transition.[17]

Another important feature of the FC curve in Fig. 1 is the small magnetic moment of only $0.33\mu_B$/Mn at 4.2 K. This value has to be compared to $(4-0.06)\mu_B$/Mn $= 3.94\mu_B$/Mn in the case of parallel spin alignment. In this context we note that demagnetizing fields $H_D = NM$ do not play an important role, because of the small susceptibility and the small magnetization M of $La_{0.94}Sr_{0.06}MnO_3$ at 4.2 K and $\mu_0 H_{ext} = 0$ T (see Fig. 3). Therefore, the presence of a small magnetic moment at low temperatures also signals competing ferro- and antiferromagnetic correlations as already mentioned above. Assuming that there is a homogeneous phase this can be understood as follows: by introducing holes into the undoped, antiferromagnetic $LaMnO_3$ compound, the isotropic ferromagnetic double-exchange (DE) mechanism[23] becomes more important. In a homogeneous phase this alters the antiferromagnetic *A*-type structure by canting the magnetic moments of adjacent lattice planes. This canting leads to a small effective magnetization and therefore represents a possible explanation of the observed small magnetic moment. On the other hand, the small magnetic moment also can be understood within the phase separation scenario. Here, both ferromagnetic and antiferromagnetic areas with different hole concentrations are assumed to develop at T_C. It is obvious that this results in a small effective magnetic moment. This point will be discussed in more detail in the next section, where the field dependence of the magnetization is presented.

Figure 2 shows magnetization versus temperature curves recorded at different applied magnetic fields. The curves have been measured at increasing temperature after cooling down in zero magnetic field [zero-field-cooled (ZFC) measurements[22]]. Below T_C a surprising behavior is observed. For the three different magnetic fields of 0.05, 0.06, and 0.08 T the magnetization was found to sharply increase at around 44, 56, 81, and 113 K, resulting in the steplike structure in the M vs T curves. As shown by Fig. 2, this feature is still preserved if a high negative magnetic field of -8 T is applied after cooling down at zero field before the magnetization is recorded at low field (0.05 T) with increasing temperature [after negative field (ANF) measurement]. It is most likely that such unusual temperature dependence of

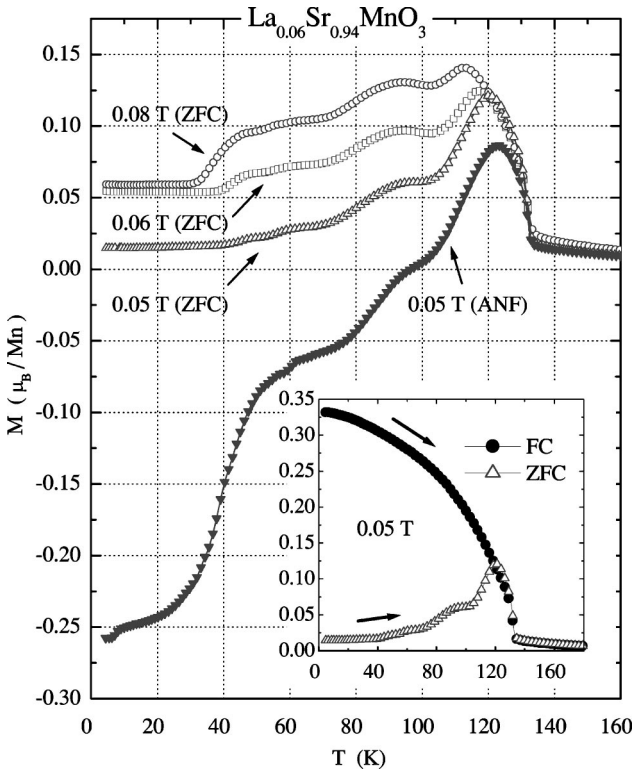

FIG. 2. Magnetization vs temperature curves (ZFC measurements) measured at different applied magnetic field obtained with increasing temperature (open symbols). The ANF curve (solid symbols) was obtained after applying a field of -8 T at 4.2 K. The inset shows a FC and a ZFC measurement for $\mu_0 H = 0.05$ T.

the magnetization results from magnetic domains present in the sample. In this case the steplike shape is expected to originate from a change in the domain structure, i.e., from collective changes of spin directions. The presence of domains is also signaled by the difference between the ZFC and the FC measurement as shown in the inset of Fig. 2.

Moreover, the comparison of the ZFC and the ANF measurements clearly demonstrates that the temperatures values, at which the steplike changes of the magnetization occurs, are not influenced by applying external magnetic fields. Figure 2 clearly shows that these temperatures values are the same for the ZFC and the ANF measurements. This strongly suggests that the magnetic domain structure is tightly linked, besides to magnetic fields, to another sample property. One likely possibility is the coupling to the lattice, mediated by the presence of twin domains: Due to a significant magnetic anisotropy, which is known to exist in the investigated material from recent neutron scattering experiments,[13,16] different twin domains correspond to different spin orientations, resulting in a magnetic domain structure. Within this picture the steplike features in the magnetization versus temperature curves are related to the collective spin reorientation of different twin domains. Such an orientation change is expected to occur, when the external magnetic field together with the thermal energy is sufficient to overcome the energy barrier due to the magnetic anisotropy. This scenario is strongly supported by a comparison of our data with magnetization measurements on an untwinned $LaMnO_3$ single crystal.[17] In the

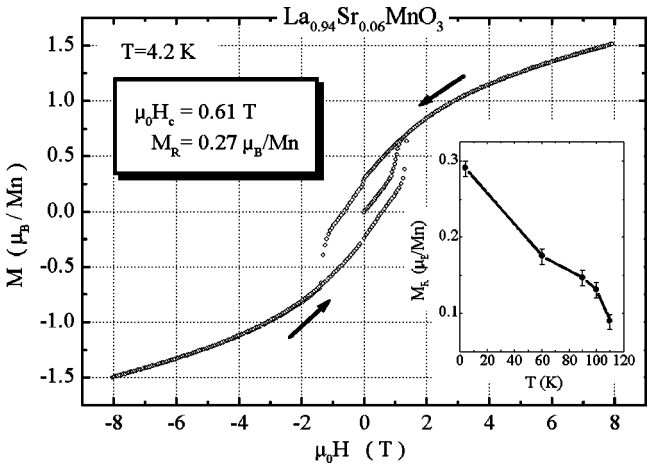

FIG. 3. Magnetization vs applied field curve of $La_{0.94}Sr_{0.06}MnO_3$ at $T=4.2$ K. The inset shows the temperature dependence of the remanent magnetization.

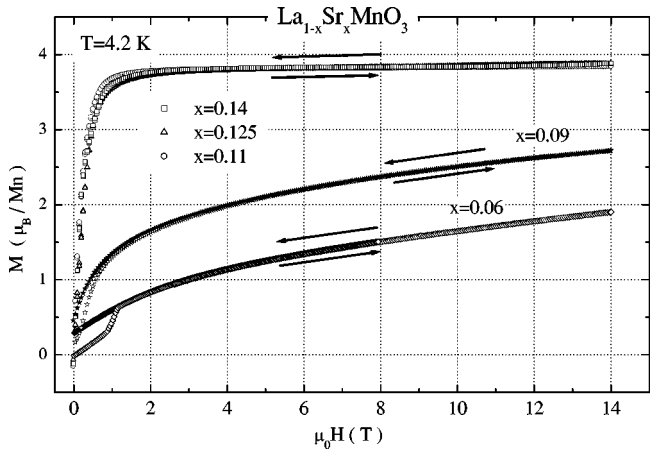

FIG. 4. Comparison between the magnetization vs applied field curves of $La_{1-x}Sr_xMnO_3$ with $x=0.06$, 0.09, 0.11, 0.125, and 0.14 at $T=4.2$ K. In contrast to $x=0.06$ and $x=0.09$ the higher-doped ferromagnetic samples do not show any hysteretic behavior.

FC mode the temperature dependence of the magnetization is qualitatively the same for the untwinned $LaMnO_3$ single crystal and our sample. However, in the ZFC mode the measured magnetization versus temperature curves of the untwinned sample show no steps. This comparison strongly suggests that the steplike features found in our measurements indeed result from the existence of different twin domains.[24]

IV. MAGNETIZATION VERSUS APPLIED MAGNETIC FIELD

We now discuss the magnetic field dependence of the magnetization at low temperatures. The magnetization versus applied magnetic field curve of $La_{0.94}Sr_{0.06}MnO_3$ measured at 4.2 K in the field range from -8 to $+8$ T is shown in Fig. 3. The data were taken after cooling the sample in zero magnetic field. Figure 3 shows a pronounced hysteresis loop, which is continuously reduced with increasing temperature (see inset of Fig. 3). At 4.2 K the measured remanent magnetization is $M_R=0.27\mu_B$/Mn and the coercive field is $\mu_0 H_c=0.611$ T. Such a high coercive field at 4.2 K cannot be caused by the pinning of magnetic domain walls alone, since the typical coercive field due to this effect is less than 0.03 T.[25] Therefore, we can conclude that the strong coercive force mainly results from the magnetic anisotropy. Magnetic anisotropy also can naturally explain the steplike increase of the magnetization at the critical field $\mu_0 H_{\rm crit}=\pm 1.2$ T (see Fig. 3). It is obvious that the system can overcome the energy barrier originating from the anisotropy at the applied field for which $\mu_0 H_{crit} M \sim K$, where K represents the anisotropy energy. We mention again that a magnetic anisotropy also generates a coupling to the lattice domain structure, i.e., does also qualitatively explain the unusual temperature dependence of the magnetization discussed in the previous section.

We first discuss the experimental observations within the PS scenario. In this scenario the shape anisotropy of the ferromagnetic regions is expected to result in a high coercive force, since the magnetization curves of the ferromagnetic samples with larger doping level do not show any hysteretic behavior at 4.2 K as demonstrated in Fig. 4. Therefore, in the following we take only into account shape anisotropy.

Starting from the antiferromagnetic A-type structure consisting of ferromagnetic ab planes coupled antiferromagnetically along the c axis, it is most reasonable to assume confined ferromagnetic areas, which have the shape of oblate spheroids (disks). This is also suggested by recent neutron scattering experiments, which give evidence for a shape elongated in the ferromagnetic ab plane and compressed along the c axis.[13] However, the magnetization curve of such a ferromagnetic region shows no hysteresis.[25] In the case of an oblate spheroid, the magnetization direction would be within the equatorial plane, i.e., perpendicular to its polar axis. If the magnetic field is applied along the polar axis, this would produce a reversible rotation of the magnetization vector out of the equatorial plane. Moreover, if one applies the field perpendicular to the polar axis, the magnetization vector can rotate freely in the equatorial plane when the magnetic field reverses its direction. As a consequence, the magnetization versus applied magnetic field curve of a oblate spheroid can only show a jump at $\mu_0 H=0$ T, but no hysteresis. Let us now consider the case of a prolate spheroid (cigar). If the ferromagnetic regions would have this shape, a hysteresis in the magnetization curve could be observed.[25] For a prolate spheroid with polar axis A and equatorial axis B the maximum coercive force is given by

$$H_c^{max}=(N_B-N_A)M_0,$$

where $N_{A,B}$ are the demagnetization coefficients corresponding to the axes A,B and M_0 is the saturated magnetization of the ferromagnetic region. With this equation it is possible to estimate H_c^{max} using $N_A+2N_B=1$ for the general spheroid with principal axes A and B. One obtains

$$\mu_0 H_c^{max} \leqslant \mu_0 \frac{1}{2}(1-3N_A)M_0 \leqslant \frac{1}{2}\mu_0 M_0 \leqslant 0.4\text{T},$$

if $M_0 = 4\mu_B$/Mn is assumed for the ferromagnetic region. This value is well below the measured coercive field and corresponds to the limit of an infinitely thin and long rod with the field applied parallel to its axis. For any more isotropic shape the expected value ranges between these two extreme limits (plane and rod). That is, the coercive field due to the corresponding shape anisotropy should be always less than 0.4 T. Therefore, our analysis demonstrates that the observed coercive field cannot be explained within the framework of an inhomogeneous phase consisting of antiferromagnetic and ferromagnetic regions. We hence can conclude that the presence of such a PS is very unlikely in the investigated sample.

We next discuss the experimental data within the CAF model, which naturally can explain the experimental observations. In order to demonstrate this in detail, we first discuss a mean-field model for CAF with anisotropy at $T = 0$ K. For this model the effective energy density for a single domain in reduced units is given by

$$\eta = a\cos\Theta - h_{DE}\cos\frac{\Theta}{2} - h_{ext}\hat{\mathbf{M}}\cdot\hat{\mathbf{H}}\cos\frac{\Theta}{2} + \sin^2\vartheta.$$

Here a is a constant describing the antiferromagnetic correlations between the adjacent ab planes, Θ the angle between the magnetization of adjacent ab planes, and h_{DE} the effective field describing the DE. The reduced field h_{ext} represents the applied magnetic field, $\hat{\mathbf{M}}$ and $\hat{\mathbf{H}}$ are the unit vectors of the magnetization and the applied field, and ϑ is the angle between the c axis and the magnetization direction (see inset of Fig. 6). In the above expression the first term describes the antiferromagnetic coupling between adjacent ab planes, which leads to the A-type AF structure of $LaMnO_3$. The second term describes the DE interaction, which is introduced by doping. The third term stands for the interaction with the external field and the last term describes the anisotropy. This form for the anisotropy energy is chosen in order to obtain a resulting ferromagnetic moment in the c direction, which is found in neutron investigations.[16]

A first result which follows from the model is the relation

$$\frac{\partial}{\partial h_{ext}}\cos\frac{\Theta}{2} = \frac{1}{4A},$$

i.e., a constant high field susceptibility at $T = 0$ K. This was also found in the analysis of De Gennes[19] and is in agreement with our experimental result obtained at $T \neq 0$ K shown in Fig. 5. In particular, the measurement at 4.2 K shows an almost linear field dependence of the magnetization for $\mu_0 H_{ext} > 8$ T.

For a further analysis of the CAF model we have calculated the magnetization curve resulting from the minimization of η. The result obtained by applying numerical techniques is shown in Fig. 6. We note that the theoretical curve was obtained by considering a twinned crystal. As already mentioned above the [001] direction, the [110] direction, as well as the a and b axes, can be interchanged and the resulting magnetization is the sum of these different contributions. The parameters of the above mean-field model are determined by fitting the susceptibility in high-field regime, the remanent magnetization, the coercive field, and the field strength H_{crit}.[26] The fitting procedure gives an anisotropy energy of

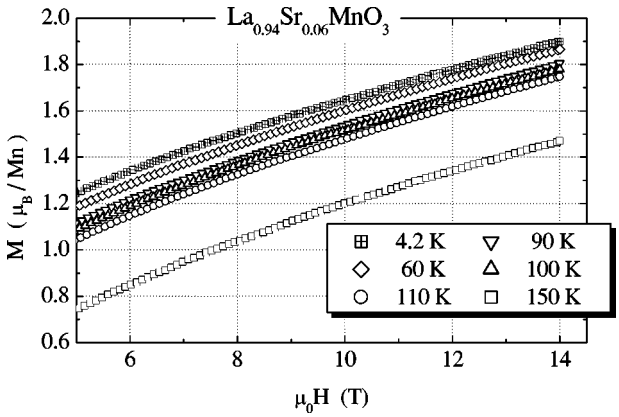

FIG. 5. Magnetization vs applied magnetic field curves of $La_{0.94}Sr_{0.06}MnO_3$ up to high-field values recorded at different temperatures. For $T = 4.2$ K a nearly linear field dependence is found.

$$K = 0.1 \quad \text{meV/Mn},$$

which is in fair agreement with the value of 0.15 meV/Mn found for $La_{0.95}Ca_{0.05}MnO_3$ in neutron scattering experiments.[16] Furthermore, the mean-field calculation leads to different susceptibilities in the low- and high-field regimes. These different susceptibilities are the result of different processes contributing to the magnetization change (see insets of Fig. 6).

In the low-field regime the canting angle Θ is almost constant and the main contribution to the susceptibility originates from a reversible change of ϑ in the domains, where the [110] direction is parallel to the applied field. In the high-field regime, where the resulting magnetization is almost parallel to the applied field, the susceptibility is due to the change of Θ.

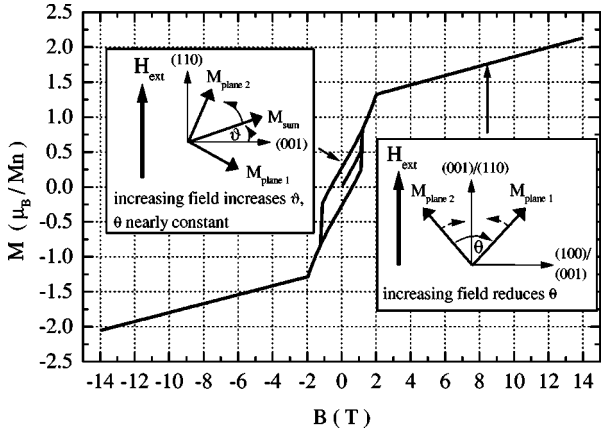

FIG. 6. Calculated magnetization vs applied magnetic field curve for a twinned single crystal using the CAF model with anisotropy. The insets show the two different processes causing the dominating magnetization change in the low- and high-field regimes as indicated by the arrows.

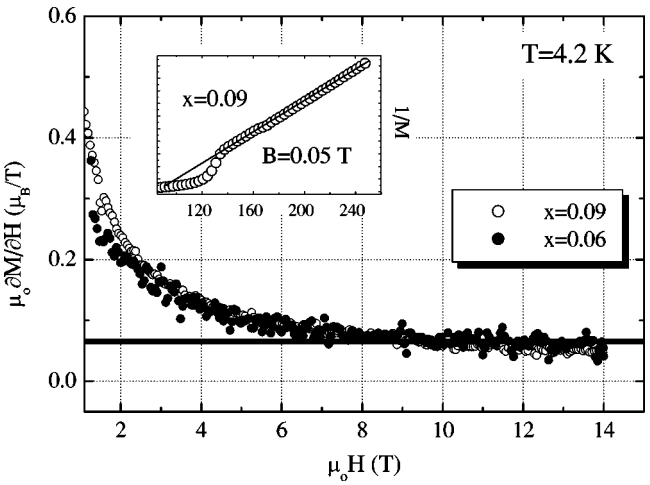

FIG. 7. Comparison between the differential susceptibilities of $La_{1-x}Sr_xMnO_3$ with $x=0.06$ and $x=0.09$ which are almost constant above 8 T. The inset displays the temperature dependence of the inverse magnetization for $x=0.09$ (compare Fig. 1).

The result of our calculation is in good agreement with the measurement shown in Fig. 3. In the low-field regime (below 1 T) we observe a higher susceptibility than in the high-field regime (above 5 T). Furthermore, we have found reversible processes below 1 T, which can be attributed to the reversible changes in ϑ mentioned above.

The pronounced kink in the calculated magnetization versus applied field curve at about 2 T originates from the specific form $K\sin^2\vartheta$ of the anisotropy energy and the fact that the theoretical curve is calculated for $T=0$ K. Further differences between theory and experiments, such as the observation of two different critical fields H_{crit} in the measured curve, can be attributed to the presence of further magnetic domains, which are not included in the calculations.

Finally, we mention that the hysteresis loop at 4.2 K of the sample with 9% strontium doping is quite similar to the one of $La_{0.94}Sr_{0.06}MnO_3$. In particular, the magnetization versus applied field curve of $La_{0.91}Sr_{0.09}MnO_3$ shows also a hysteresis (Fig. 4). Moreover, as demonstrated in Fig. 7, the differential susceptibility $\partial M/\partial H$ versus applied field curves are almost the same above 1.5 T, including the nearly constant high-field susceptibility which is characteristic for the CAF state. Moreover, the temperature-dependent inverse magnetization of $La_{0.91}Sr_{0.09}MnO_3$ and $La_{0.94}Sr_{0.06}MnO_3$ is qualitatively the same, as can be seen by comparing the data shown in the insets of Fig. 1 and Fig. 7. These striking similarities of the field- and temperature-dependent magnetization strongly suggest that the sample with 9% strontium doping is also in a CAF state at low temperatures. The observed coercive force of $\mu_0 H_c \simeq 0.2$ T, i.e., the smaller anisotropy, and the increased magnetization compared to the sample with 6% strontium doping can naturally be explained by the ferromagnetic isotropic double-exchange mechanism which increases with growing strontium content.

V. CONCLUSION

Focusing on a $La_{0.94}Sr_{0.06}MnO_3$ crystal we have investigated the temperature and magnetic field dependence of lightly doped manganites. In case of $x=0.06$ the comparison between ZFC, FC, and ANF measurements recorded at increasing temperature gives clear evidence for the existence of different magnetic domains. Furthermore, our measurements strongly suggest that the magnetic domains are strongly coupled to the twin domains of the lattice.

We have presented a detailed analysis of the corresponding magnetization curve at 4.2 K, which shows a pronounced hysteresis. From this analysis we can conclude that this hysteresis is not caused by domain wall motion, since in this case a much smaller coercive field is expected. Furthermore, we can rule out a phase separation into ferromagnetic and antiferromagnetic regions for the same reason. On the other hand, we have shown that a CAF model reproduces the main features of the measured magnetization versus applied magnetic field curves, namely, a constant high-field susceptibility, a remanent magnetization, a large coercive force, and a jumplike increase of the magnetization at the critical field H_{crit}. Therefore, our analysis strongly suggests the presence of a homogeneous CAF phase. The doping regime of the homogenous CAF phase extends at least up to 9% strontium doping, as demonstrated by the magnetization versus applied field curves of $La_{1-x}Sr_xMnO_3$ with $0.06 \leqslant x \leqslant 14$.

ACKNOWLEDGMENTS

The authors acknowledge useful discussion with S. Uhlenbruck and would like to thank B. Herrero-Aldea for a critical reading of the manuscript. This work was supported by the Deutsche Forschungsgemeinschaft.

*Present address: II. Physikalisches Institut, RWTH Aachen, 52056 Aachen, Germany.

†Present address: Walther-Meissner-Institut, Bayerische Akademie der Wissenschaften, 84748 Garching, Germany.

[1] D.I. Khomskii and D.I. Sawatzky, Solid State Commun. **102**, 87 (1997).

[2] S. Uhlenbruck, R. Teipen, R. Klingeler, B. Büchner, O. Fried, M. Hücker, H. Kierspel, T. Niemöller, L. Pinsard, A. Revcolevschi, and R. Gross, Phys. Rev. Lett. **82**, 185 (1999).

[3] J.C. Irwin, J. Chrzanowski, and J.P. Franck, Phys. Rev. B **59**, 9362 (1999).

[4] H.Y. Hwang, S.-W. Cheong, P.G. Radaelli, M. Marezio, and B. Batlogg, Phys. Rev. Lett. **75**, 914 (1995).

[5] H. Kawano, R. Kajimoto, M. Kubota, and Y. Yoshizawa, Phys. Rev. B **53**, 14 709 (1996).

[6] T. Niemöller, M. v. Zimmermann, S. Uhlenbruck, O. Friedt, B. Büchner, T. Frello, N.H. Andersen, P. Berthet, L. Pinsard, A.M. De Leon-Guevara, A. Revcolevschi, and J.R. Schneider, Eur. Phys. J. B **8**, 5 (1999).

[7] Y. Yamada, O. Hino, S. Nohdo, R. Kanao, T. Inami, and S. Katano, Phys. Rev. Lett. **77**, 904 (1996).

[8] Y. Endoh, K. Hirota, S. Ishihara, S. Okamoto, Y. Murakami, A. Nishizawa, T. Fukuda, H. Kimura, H. Nojiri, K. Kraneko, and S. Maekawa, Phys. Rev. Lett. **82**, 4328 (1999).

[9] Y. Murakami, J.P. Hill, D. Gibbs, M. Blume, I. Koyama, M. Tanaka, H. Kawata, T. Arima, Y. Tokura, H. Hirota, and Y. Endoh, Phys. Rev. Lett. **81**, 582 (1998).
[10] G. Papavassiliou, M. Fardis, M. Belesi, M. Pissas, I. Panagiotopoulos, G. Kallias, D. Niarchos, C. Dimitropoulos, and J. Dolinsek, Phys. Rev. B **59**, 6390 (1999).
[11] S. Yunoki, A. Moreo, and E. Dogotto, Phys. Rev. Lett. **81**, 5612 (1998).
[12] E.L. Nagaev, Phys. Rev. B **58**, 816 (1998).
[13] M. Hennion, F. Moussa, G. Biotteau, J. Rodriguez-Carvajal, L. Pinsard, and A. Revcolevschi, Phys. Rev. B **61**, 9513 (2000).
[14] G. Allodi, R. De Renzi, G. Guidi, F. Licci, and M.W. Pieper, Phys. Rev. B **57**, 1024 (1998).
[15] K. Kumagai, A. Iwai, Y. Tomoika, H. Kuwahara, Y. Tokura, and A. Yabukovskii, Phys. Rev. B **59**, 97 (1999).
[16] F. Moussa, M. Hennion, G. Biotteau, J. Rodriguez-Carvajal, L. Pinsard, and A. Revcolevschi, Phys. Rev. B **60**, 12 299 (1999).
[17] V. Skumryev, F. Ott, J.M.D. Coey, A. Anane, J.-P. Renard, L. Pinsard-Gaudart, and A. Revcolevschi, Eur. Phys. J. B **11**, 401 (1999).
[18] A. Pimenov, M. Bibermacher, D. Ivannikov, A. Loidl, V.Y. Ivanov, A.A. Mukhin, and A.M. Balbashov, Phys. Rev. B **62**, 5685 (2000).
[19] P.-G. De Gennes, Phys. Rev. **118**, 141 (1960).
[20] M. Paraskevopoulos, F. Mayr, J. Hemberger, A. Loidl, R. Heichle, D. Maurer, V. Müller, A.A. Mukhin, and A.M. Balbashov, J. Phys.: Condens. Matter **12**, 3993 (2000).
[21] A. Revcolevschi and G. Dhalenne, Adv. Mater. **5**, 657 (1993).
[22] In FC measurements the sample is cooled down in the external magnetic field from about 200 K to 4.2 K. Then the measurement of the magnetization is performed at increasing temperature. In ZFC measurements the sample is cooled down in zero magnetic field.
[23] C. Zener, Phys. Rev. **82**, 403 (1951).
[24] On the basis of our magnetization data we cannot definitely say what the microscopic magnetizations processes are which lead to the observed $M(T)$ curves. However, the relation between the steplike shape and the twin domains is quite apparent by the comparison of our data with that of an untwinned crystal (Ref. 17). Since the magnetic properties of $La_{1-x}Sr_xMnO_3$ are known to be strongly coupled to the lattice (Ref. 5), one possible origin for the steplike shape of the $M(T)$ curves might be the different strain on the different lattice domains of the twinned sample.
[25] E.C. Stoner, Rep. Prog. Phys. **13**, 83 (1950).
[26] In the CAF model the critical field H_{crit} is given by $\mu_0\vec{H}_{crit}\cdot\vec{M} = \mu_0 H_{crit}(4\mu_B\cos\Theta/2) = K/2$, where M is the magnetization in domains with the [001] direction parallel to the field. At this field the jumplike changes of the field-dependent magnetization occur.